

## Supporting information

### Synergistic Optimization of Composition-Structure-Conductive Network for High-Performance Integrated Transition Metal Oxide Anodes for Lithium-Ion Batteries

Qiang Ma, Junwei Sha, Biao Chen, Enzuo Liu, Chunsheng Shi, Liying Ma, Fang He,  
Chunnian He, Naiqin Zhao, Jianli Kang\*

Q. Ma, C. He, B. Chen, L. Ma, N. Zhao, J. Kang  
School of Materials Science and Engineering,  
Tianjin University, Tianjin, 300350, P.R. China  
State Key Laboratory of Precious Metal Functional Materials,  
Tianjin University, Tianjin, 300350, P.R. China  
National Industry-Education Platform of Energy Storage,  
Tianjin University, 135 Yaguan Road, Tianjin 300350, P.R. China  
E-mail: [jianlikang@tju.edu.cn](mailto:jianlikang@tju.edu.cn)

C. Shi, J. Sha, F. He, E. Liu  
School of Materials Science and Engineering,  
Tianjin University, Tianjin, 300350, P.R.  
China State Key Laboratory of Precious Metal Functional Materials,  
Tianjin University, Tianjin, 300350, P.R. China

#### 1. Supporting Figures

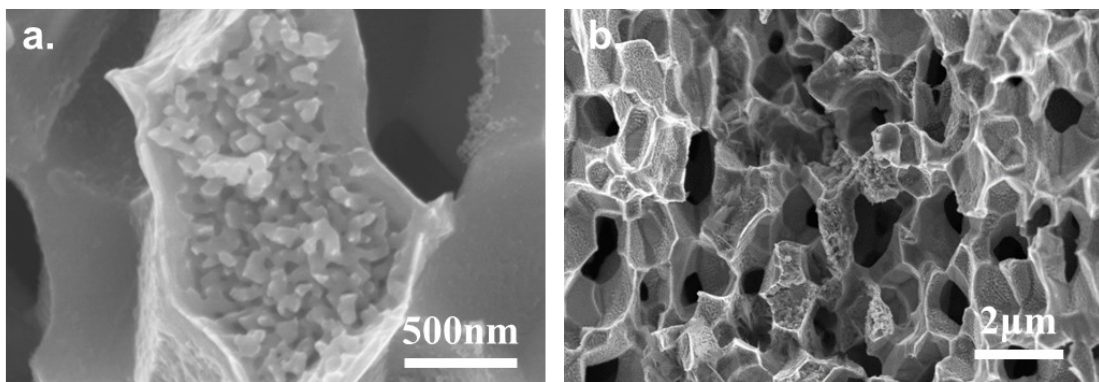


Fig. S1. The structure of hp-CM

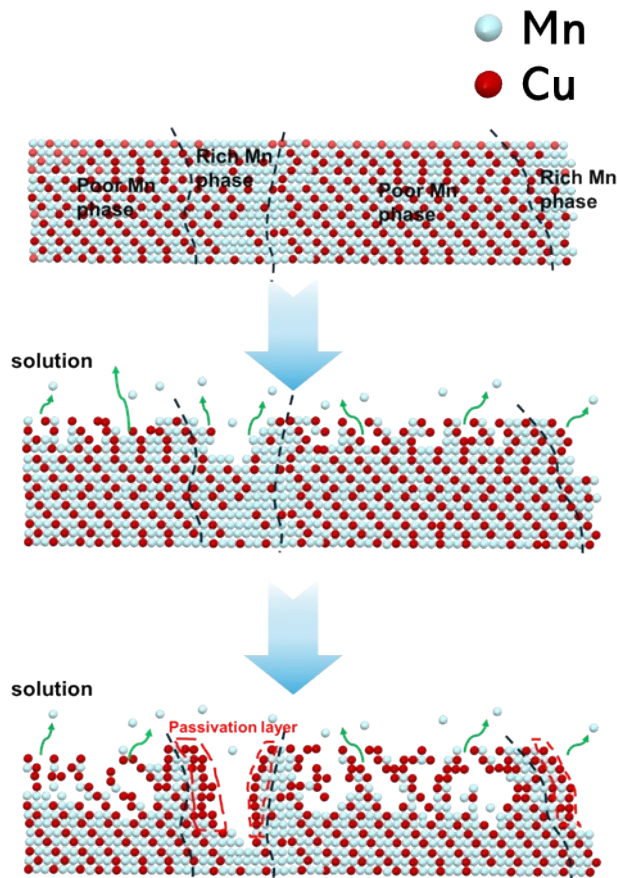


Fig. S2. Description of dealloying process about hp-CM

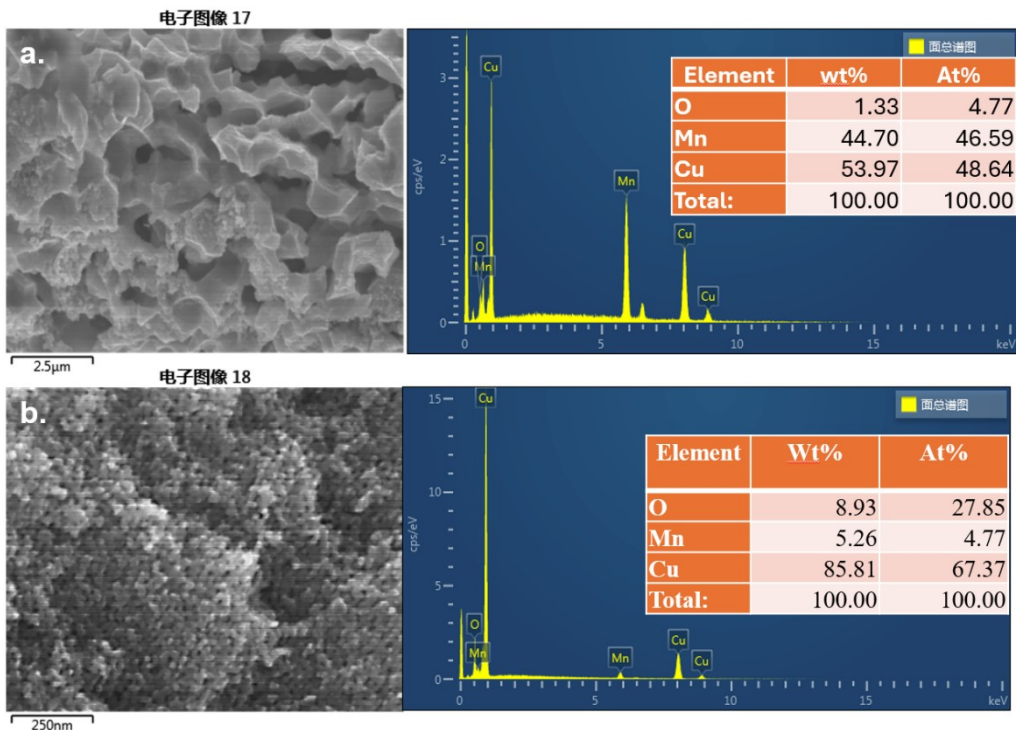


Fig. S3. The structure and chemical composition of a) hp-CM and b) np-CM

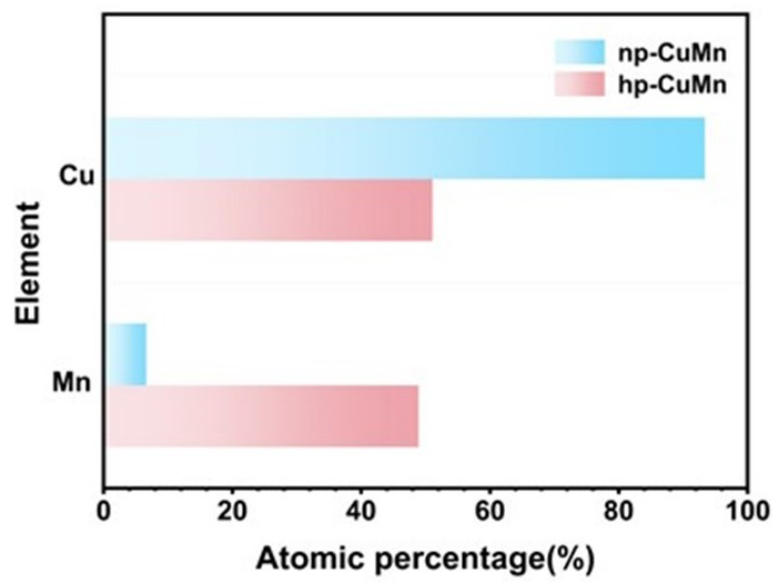


Fig. S4. Comparison of elemental composition between np-CM and hp-CM

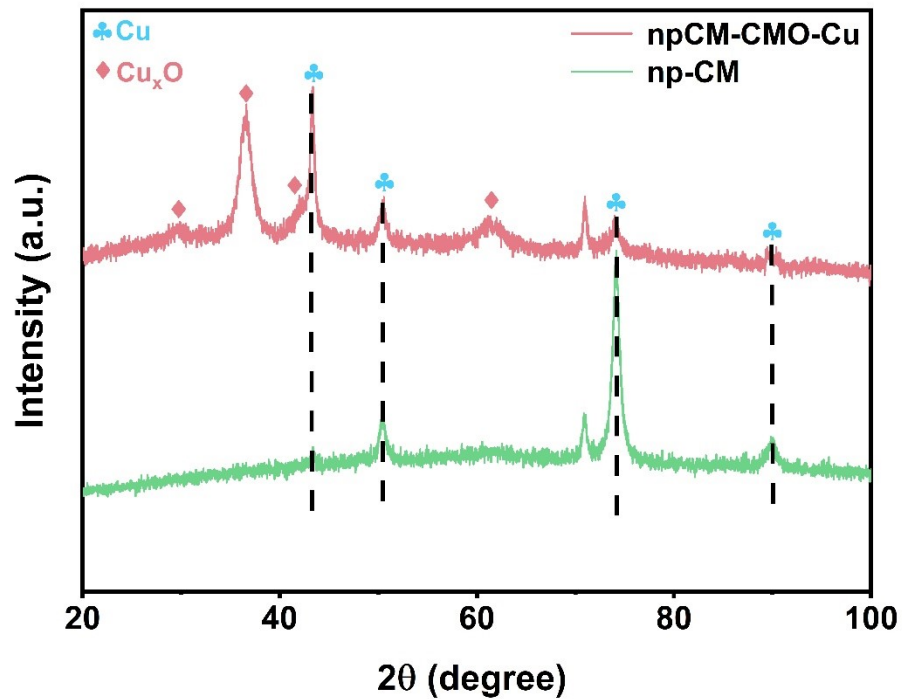


Fig. S5. XRD patterns of np-CM and npCM-CMO-Cu

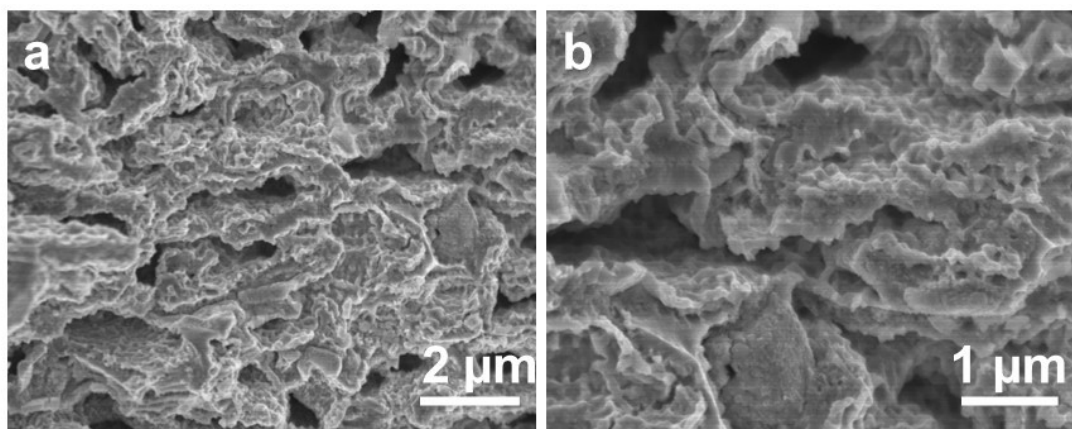


Fig. S5. SEM images of hpCM@CMO

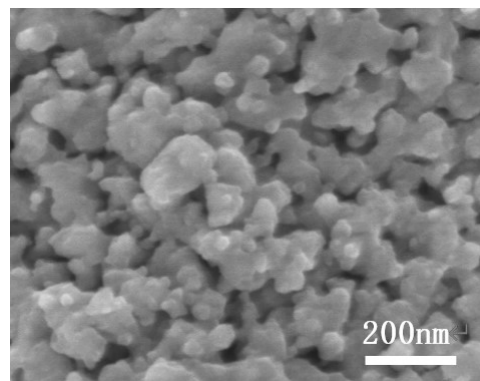


Fig. S6. SEM images of npCM-CMO-Cu

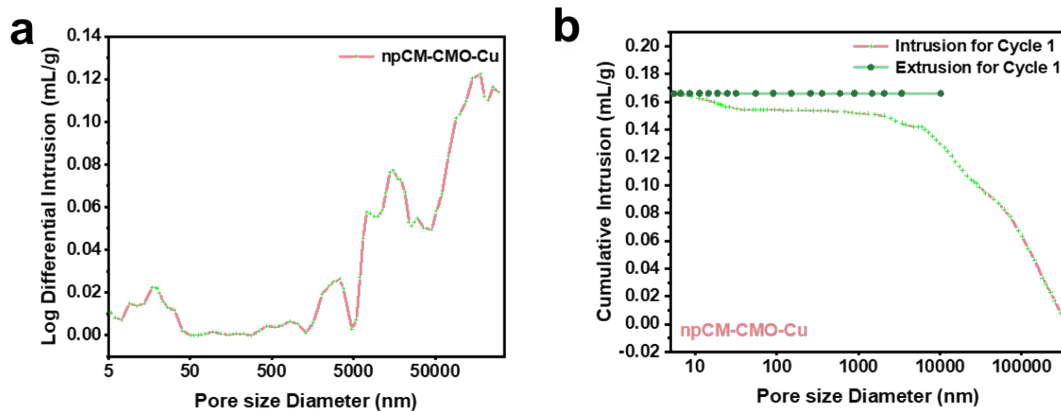


Fig. S7 MIP patterns of npCM-CMO-Cu electrode. a) Log Differential Intrusion vs Pore size and b) Cumulative Intrusion vs Pore size of npCM-CMO-Cu.

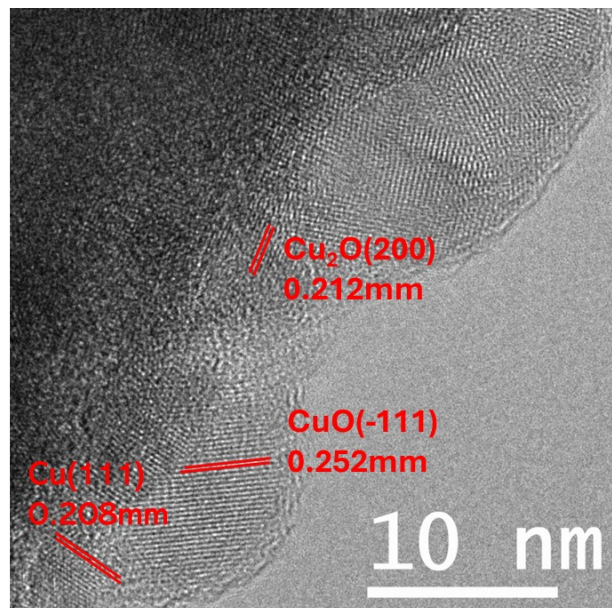


Figure S8 HRTEM images of hpCM-CMO-Cu.

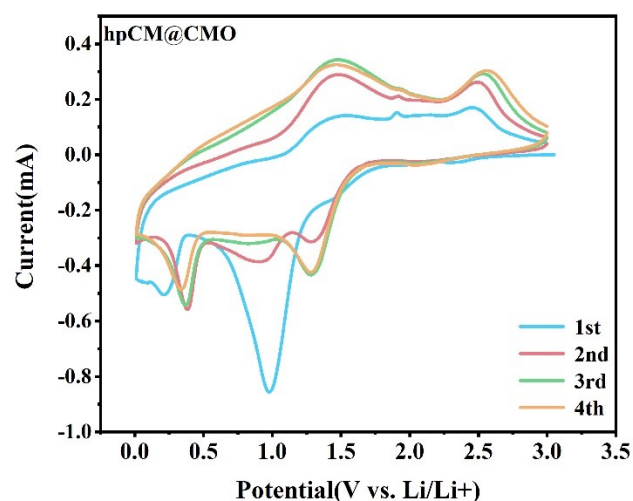


Fig. S9. CV curves of hpCM@CMO electrode at  $0.2 \text{ mV s}^{-1}$

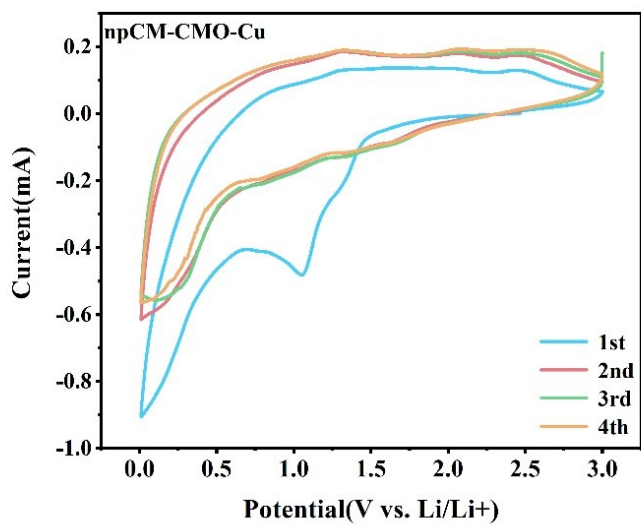


Fig. S10. CV curves of npCM-CMO-Cu electrode at  $0.2 \text{ mV s}^{-1}$

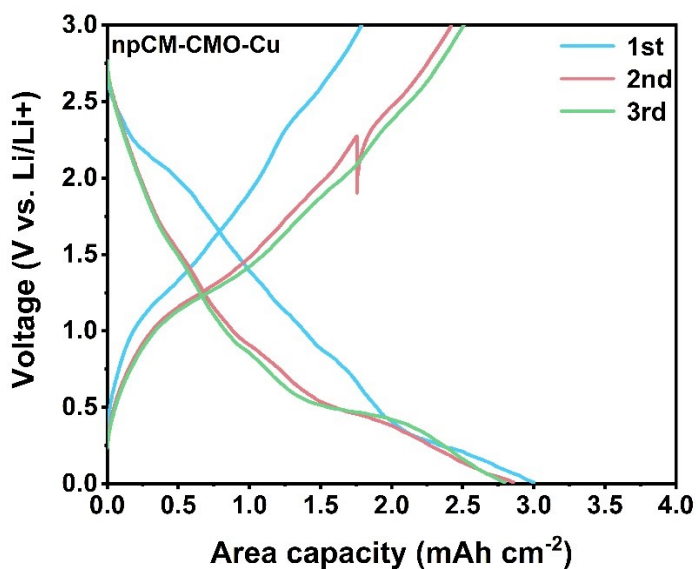


Fig. S11. Galvanostatic charge - discharge profiles of npCM-CMO-Cu electrode at  $0.4 \text{ mA cm}^{-2}$

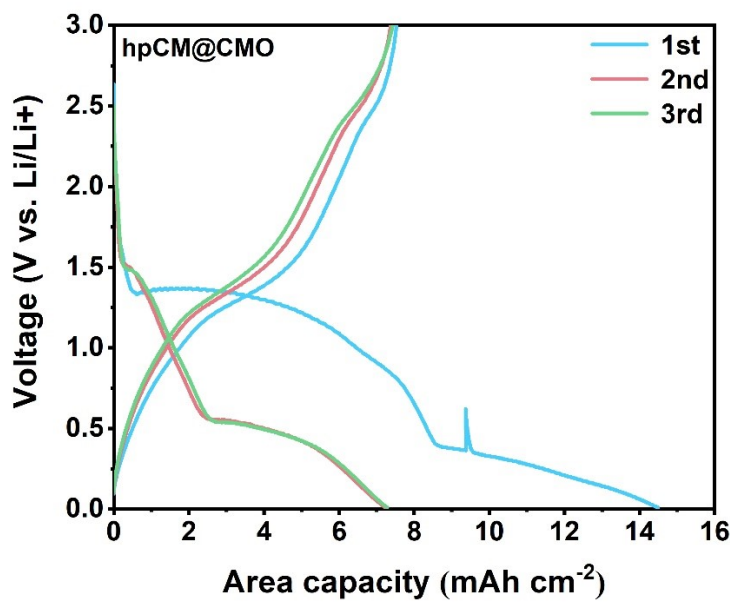


Fig. S12. Galvanostatic charge – discharge profiles of hpCM@CMO electrode at 0.4 mA cm<sup>-2</sup>

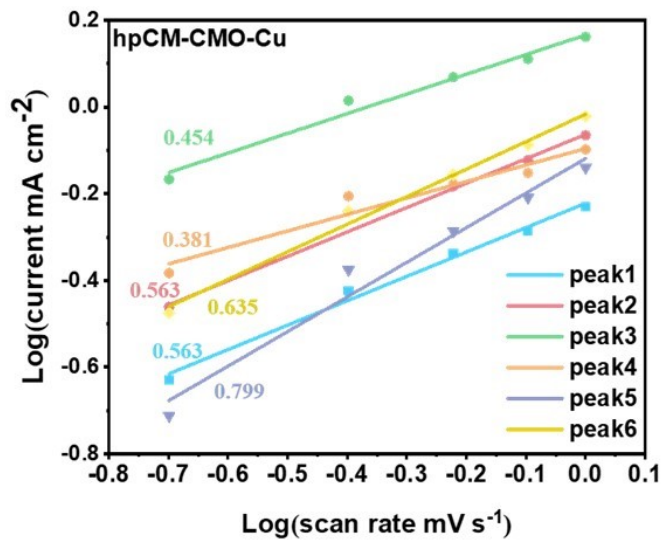


Fig. S13. Linear relationship between log(i) and log(v).

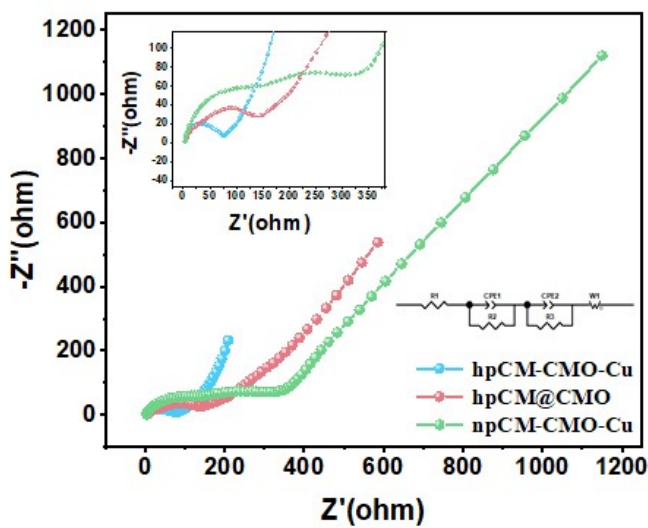


Fig. S14. EIS spectra of hp-CM, hpCM@CMO, and npCM-CMO-Cu after 50<sup>th</sup> cycles.

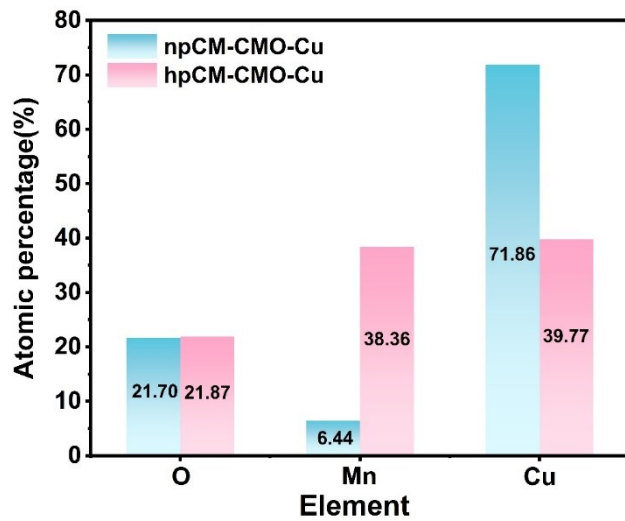


Fig. S15. Comparison of elemental composition between hpCM-CMO-Cu and npCM-CMO-Cu.

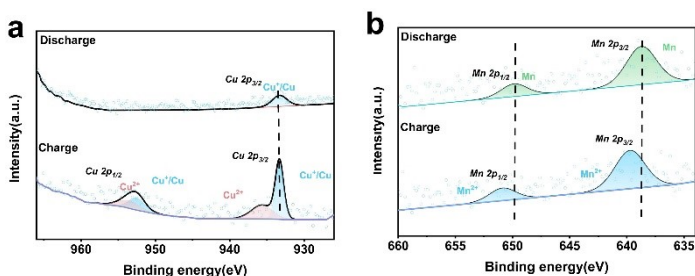


Fig S16 XPS spectra of hpCM-CMO-Cu first discharge and charge. a)Cu 2p, b)Mn 2p.

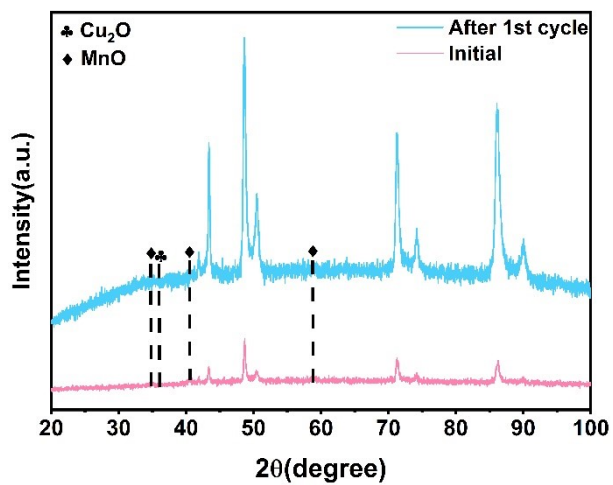


Fig. S17. XRD patterns of hpCM-CMO-Cu before and after 1<sup>st</sup> cycle.

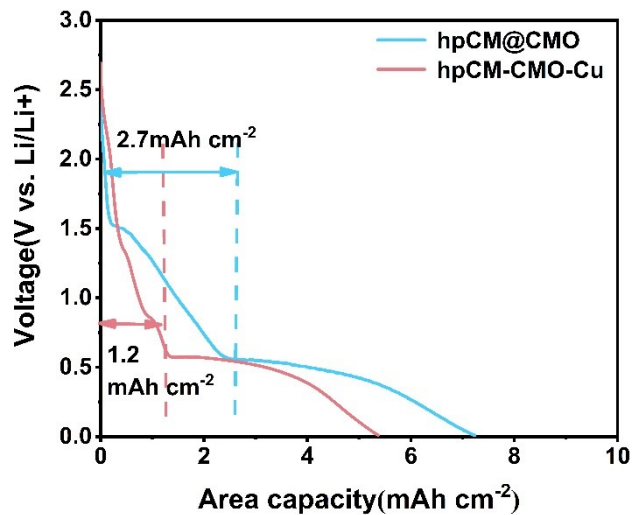


Fig. S18 Comparison of hpCM-CMO-Cu and hpCM@CMO discharge profiles.

### 3. Supporting Tables

Table S1 Pore structure comparison of hpCM-CMO-Cu and npCM-CMO-Cu

Materials	Porosity	Specific surface area (m <sup>2</sup> /g)	The average size of nanopore(nm)	The average size of submicron pore(nm)
hpCM-CMO-Cu	53.8660%	3.390	18.24	456.38
npCM-CMO-Cu	48.9512%	3.486	11.47	/

Table S2 Comparison of charge capacities of various three-dimensional self-supported oxide electrodes from the literature

Materials	active substance	Electrochemical performance			Ref.
		Current density [mA cm <sup>-2</sup> ]	Cycle number	Capacity retention [mAh cm <sup>-2</sup> ]	
hpCM@CMO	Cu <sub>x</sub> O, MnO	1	250	1.25	This work
npCM-CMO-Cu	Cu <sub>x</sub> O, MnO	1	250	0.492	This work
hpCM-CMO-Cu	Cu <sub>x</sub> O, MnO	1	250	4.38	This work
3D-HNP Cu <sub>x</sub> O@m-Cu	Cu <sub>x</sub> O	1	200	2.02	1
3D-HNP SnO <sub>2</sub> /CuxO@n-Cu	Cu <sub>x</sub> O, SnO <sub>2</sub>	1	200	3.34	2
3D NPCu@Cu <sub>2</sub> O	Cu <sub>2</sub> O	0.175	120	1.45	3
3D NPC@1D Cu <sub>2</sub> O NWN	Cu <sub>2</sub> O	0.1	150	1.64	4
nanoporous Sn - Co alloy	Co <sub>3</sub> Sn <sub>2</sub>	1	200	0.89	5
ATO/CC/OTO	TiO <sub>2</sub> , MnO,	1.6	140	~2.2	6
MnO/3DGS	Fe <sub>3</sub> O <sub>4</sub>	4.16	1000	1.57	7
MF-P 700	MnO, Fe <sub>3</sub> C	0.4	250	0.97	8



## References

1. X. M. Yan, H. Kang, P. Cheng, S. C. Zhang, S. Q. Shi and W. B. Liu, *EcoMat*, 2022, **4**, e12208.
2. X. M. Yan, W. B. Liu, H. Kang, S. C. Zhang and S. Q. Shi, *Advanced Functional Materials*, 2023, **33**, 2212654.
3. D. Q. Liu, Z. B. Yang, P. Wang, F. Li, D. S. Wang and D. Y. He, *Nanoscale*, 2013, **5**, 1917-1921.
4. W. B. Liu, L. Chen, L. Cui, J. Z. Yan, S. C. Zhang and S. Q. Shi, *Journal of Materials Chemistry A*, 2019, **7**, 15089-15100.
5. H. Kang, H. Y. Liu, H. M. Gou, S. C. Zhang and W. B. Liu, *Journal of Materials Chemistry A*, 2024, **12**, 21723-21731.
6. L. Luo, K. Liang, Z. Khanam, X. C. Yao, M. Mushtaq, T. Ouyang, M. S. Balogun and Y. X. Tong, *Small*, 2024, **20**, 2307103.
7. P. H. Chen, W. Y. Zhou, Z. J. Xiao, S. Q. Li, H. L. Chen, Y. C. Wang, Z. B. Wang, W. Xi, X. G. Xia and S. S. Xie, *Energy Storage Materials*, 2020, **33**, 298-308.
8. F. Xie, X. L. Sheng, Z. B. Ling, S. J. Hao, Q. Y. Zhang, M. Sun, G. T. Liu, F. Y. Diao and Y. Q. Wang, *Electrochimica Acta*, 2023, **470**, 143288.